FTD-ID(RS)T-0712-89

FOREIGN TECHNOLOGY DIVISION

APPLICATIONS OF ACOUSTO-OPTICAL CORRELATION DEVICES IN RADAR SIGNAL PROCESSING

by

Xu Jieping, Yu Kuanxin

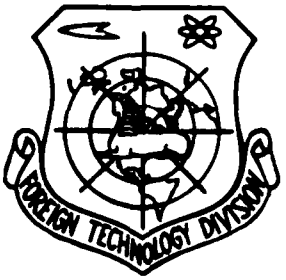

Approved for public release;
Distribution unlimited.

HUMAN TRANSLATION

FTD-ID(RS)T-0712-89 29 September 1989

MICROFICHE NR: FTD-89-C-000802

APPLICATIONS OF ACOUSTO-OPTICAL CORRELATION DEVICES IN RADAR SIGNAL PROCESSING

By: Xu Jieping, Yu. Kuanxin

English pages: 13

Source: Applied Acoustics, Vol. 5, Nr. 1, January 1986, pp. 1-5

Country of origin: China
Translated by: SCITRAN
F33657-84-D-0165
Requester: FTD/TQTR/J.M. Finley

PREPARED BY:

TRANSLATION DIVISION
FOREIGN TECHNOLOGY DIVISION
WPAFB OHIO

GRAPHICS DISCLAIMER

All figures, graphics, tables, equations, etc. merged into this translation were extracted from the best quality copy available.

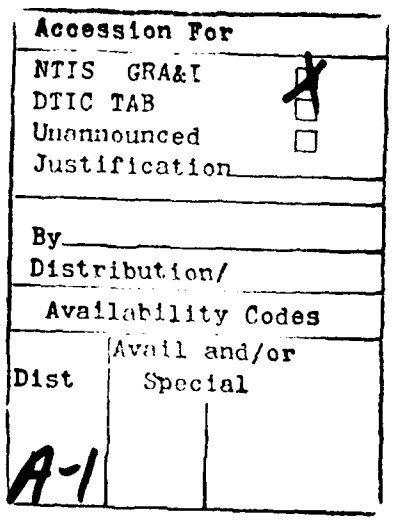

APPLICATIONS OF ACOUSTO-OPTICAL CORRELATION DEVICES IN RADAR SIGNAL PROCESSING

XU JIEPING, YU KUANXIN

This article, from the angle of experimentation, investigated the actual efficiency of acousto-optical correlation devices in radar signal processing. As far as centimeter wave band (3GHz) single carrier frequency square pulse radar signals and unmodulated random wave interference is concerned, it measured different pulse widths, different signal-to-noise ratios and, for these periods of time, the height of correlation peaks as well as the size of the correlation gain when there were different pulse widths. When the pulse width was 2.5 μs, the correlation gain was 30dB. When the pulse width was 0.5 μs, the correlation gain was 23dB. As far as the correlation peaks of acousto-optical correlation device outputs are concerned, they were all several score mV or higher. It was not necessary to go through any amplification. Rather, it was possible to make use of an oscillascope to directly carry out obsevations and measurements.

I. Introduction

As far as raising the signal-to-noise ratio of radar signals and increasing their anti-static capabilities is concerned, all through history, this has been one of the basic problems in radar signal processing. Speaking from the point of view of theory, correlation reception is capable of reaching a theoretical maximum signal-to-noise ratio. Moreover, it is easy to realize this. Because of this fact, early on, there were already people discussing acousto-optical correlation devices and the possibility of using them in the processing of radar signals [1]. Due to the fact that in the first half of the 1970's, the capabilities of acousto-optical components saw a very large increase, as a result, in the last half of the 1970's, acousto-optical devices received widespread interest, with many types of designs being put forward [2-3]. At the present time, spacial integral acousto-optical devices' time band width product can reach 10^4[4]. Moreover, as far as time integration acousto-optical correlation devices are concerned, due to the fact that, in theory, one could eliminate the limits of component size on time band width product limits, time band width products or integrals are capable of reaching 10^6-10^8[2]. Besides this, there were also people who

put forward designs for practically implementing acousto-optical correlation devices by the use of acoustic surface waves [5-7]. As compared to other correlation devices (or roll integrators) which have been discussed, acousto-optical correlation devices possess much larger time band width products or integrals. Moreover, correlation efficiency is very high. Output correlation peaks are all several score millivolts or more. It is not necessary to carry out any amplification. Rather, it is possible to use oscillascopes to carry out direct observations and measurements. This article, setting out from the angle of practical use, synthesizes the current actual situation. As far as the practical results of acousto-optical correlation devices used in radar signal processing are concerned, we did experimental research. We did research on four types of acousto-optical correlation devices (two types were spacial integral types and two types were time integral types). This article introduces one type of design which possesses relatively good anti-interference capabilities. Below, we will introduce the principles of this design, its apparatus, and experimental results. As far as centimeter wave band (3GHz) square pulse radar signals and unmodulated random wave interference is concerned, when the radar signal pulse width is 2.5 μ s, the correlation gain is 30dB. When the pulse width is 0.5 μ s, the correlation gain is 23dB.

II. Operating Principles

According to the definition for correlation functions

$$R_{12}(\tau) = \int_{-\infty}^{+\infty} s_1(t)s_2(t-\tau)d\tau$$

it is possible to know that correlation calculations have three basic operations: relative delay, phase multiplication, and integral. This article introduces the principles of spacial integral acousto-optical correlation devices as shown in Fig.1. Due to the fact that the first acousto-optical device component AOD_1, through lenses L_1 and L_2, forms an inverted image at the location of the second acousto-optical

component AOD_2, it follows that the ultrasonic waves set off by electrical signals $s_1(t)$ and $s_2(t)$ are propagated along the opposite direction, completing the relative delay. After the light, in continuing, passes through two acousto-optical components, the amplitude of the radiated light is determined by the product $s_1(t)$ $s_2(t-\tau)$. The lens L_3 takes the light from different spacial coordinates x and concentrates it all at a point photoelectric receiving device. Completing the integral for the spacial coorinates, it follows that the output electric current from the photoelectric receiving device will then be correlation function $R_{12}(\tau)$. It should be pointed out that spacial integral equipment (different from time integral equipment), in actuality, is a roll integral device. In order to complete the correlation, one of the signals among them [for example, $s_2(t)$], should first have its inversion selected. Of course, as far as single carrier frequency square pulse radar signals are concerned, the signal itself possesses inverse symmetry characteristics. It is then not necessary to first go through inversion. The acousto-optical components we used all were Bragg diffraction components. During actual operation, one should turn, in the direction shown by the arrow in Fig.1, through a Bragg angle, causing the two device components to both operate on +1 level Bragg diffraction. In addition, they both then satisfy the condition $k_d = k_i+k$. In this equation, k_i and k_d respectively are the wave vectors for the light radiated in and the diffracted light. Moreover, k is then the wave vector for the ultrasonic waves.

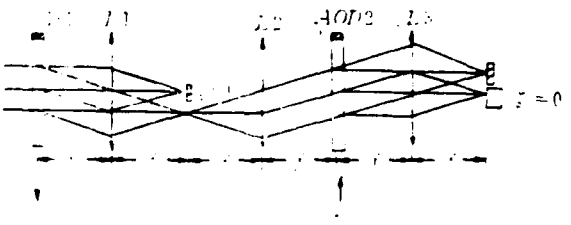

Fig.1 Diagram of Principles for Spacial Integral Acousto-Optical Correlation Device

In order, from a theoretical point of view, to do a detailed analysis of acousto-optical correlation devices, particularly in the discussion of the equipment in this article, in order to precisely specify the position of the light diaphragm on the plane ξ and the position of the point photoelectric receiving device on the plane ξ', as well as their effects, one should precisely specify the complex rate of transmission for the acousto-optical components and their physical significance. In this way, it is then possible to take the theory pertaining to acousto-optical correlation devices and analyze it into a Fourier optical theory system. As reference [8] points out, when the components operate in +1 Bragg diffraction, the rate of complex transmission for the ultrasonic waves propagated from the acousto-optical component AOD_1 along the direction of the +x axis is

$$\tilde{t}_1(x,t) = 1 + j\frac{1}{2}\tilde{g}_1(x-vt) \tag{1}$$

Moreover, the rate of complex transmission for the ultrasonic waves propagated from the acousto-optical component or device AOD_2 along the -x direction is

$$\tilde{t}_2(x,t) = 1 + j\frac{1}{2}\tilde{g}_2^*(x+vt) \tag{2}$$

In these equations, $g_1(x-vt)$ and $g_2(x+vt)$ respectively are the media refraction rate distributions given rise to by acousto-optical effects in AOD_1 and AOD_2. $\tilde{g}_1(x-vt)$ and $\tilde{g}_2(x+vt)$ are then, respectively, the complex number forms corresponding to the real distributions $g_1(x-vt)$ and $g_2(x+vt)$. Due to the fact that the adjustment of Bragg diffraction focusing is a single side band adjustment, it follows that it is necessary to select for use a complex number representation. The relationship between the refraction distributions g_1 and g_2 and the output signals $s_1(t)$ and $s_2(t)$ is very easy. From the boundary conditions

$$cs_1(t) = g_1\left(-\frac{1}{2}w - vt\right)$$

and

$$cs_2(-t) = g_2\left(\frac{1}{2}w + vt\right)$$

one obtains it (in these w is the length of the device along the direction of ultrasonic propagation). Along with this, one has

$$cs_1(t) = g_1\left[-v\left(t + \frac{T}{2}\right)\right], \qquad (3)$$
$$cs_2(t) = g_2[-v(t + T/2)]$$

In these equations, T ≡ w/v and is the ultrasonic transit time for the devices. From equation (3), it is possible to see that the distributions of the refraction rates g_1 and g_2, besides the proportionality factor -v and the fixed delay -T/2, are completely the same as the input electrical signals. Radar signals are all narrow band signals. It is possible to write

$$s(t) = a(t)\cos[2\pi f_0 t + \alpha(t)].$$

In this equation, a(t) and ∝(t) respectively are the amplitude and phase adjustments, or, written as complex signals

$$\tilde{s}(t) = \tilde{a}(t)e^{-j2\pi f_0 t}$$

In this $\tilde{a}(t) \equiv a(t)e^{-j\alpha(t)}$ and is called the complex envelope. It follows from this that the complex number representation of the refraction rate distribution is

$$\tilde{g}(x) = \tilde{a}(x)e^{j2\pi f_0 x}$$

In the equations $\xi_0 \equiv f_0/v$, that is, the null or empty frequency. In particular, one has

$$\tilde{g}_1(x - vt) = \tilde{a}_1(x - vt)e^{j2\pi\xi_0(x-vt)}$$
$$= \tilde{a}_1(x - vt)e^{j2\pi\xi_0 x}e^{-j2\pi f_0 t} \quad (4)$$

$$\tilde{g}_2^*(x + vt) = \tilde{a}_2^*(x + vt)e^{-j2\pi\xi_0(x+vt)}$$
$$= \tilde{a}_2(x + vt)e^{-j2\pi\xi_0 x}e^{-j2\pi f_0 t} \quad (5)$$

Let us assume that the light radiating in is parallel to the parallel light axis (the empty or null frequency is zero). Then, the light radiating in is of a complex amplitude which is $\tilde{u}_i = \tilde{a}_0 e^{-j2\pi ft}$.

In this, $\tilde{\tilde{a}}_0$ is a complex constant. f is the light frequency. After going through AOD_1, the complex amplitude of the light is $\tilde{u}' = \tilde{u}_i\tilde{t}_1(x,t) = \tilde{a}_0 e^{-j2\pi ft}\tilde{t}_1(x,t)$. Taking equation (1), after substituting into equation (4), one then obtains

$$\tilde{u} = \tilde{a}_0 e^{-j2\pi ft} + j\frac{1}{2}\tilde{a}_0\tilde{a}_1(x$$
$$- vt)e^{j2\pi\xi_0 x}e^{-j2\pi \cdots}$$

In this equation, the first quantity null or empty frequency is $\xi_0 = 0$. The second quantity null or empty frequency is $\xi = \xi_0$. At the position on the null or empty frequency plane where $\xi = 0$, one places a diaphragm. Then, it is possible to eliminate the first term. The equation above becomes

$$\tilde{u}' = j\frac{1}{2}\tilde{a}_0\tilde{a}_1(x - vt)e^{j2\pi\xi_0 x}e^{-j2\pi(f+f_0)t} \quad (6)$$

Again, after going through AOD_2, the complex amplitude of the light radiating out is

$$\tilde{u}_0 = \tilde{u}'\tilde{t}_2(x,t),$$

Take equation (2) and, after substituting into equation (5), one, then, obtains

$$\tilde{u}_0 = \tilde{u}' + j\frac{1}{2}\tilde{u}'\tilde{a}_2^*(x + vt)e^{-j2\pi\xi_0 x}e^{-j2\pi f_0 t}$$

After taking equation (6) and substituting in, it is easy to see that the null or empty frequency of the first term is still $\xi = \xi_0$. Moreover, the null or empty frequency of the second term is $\xi = 0$. Because of this, if one takes the point photoelectric receiving device and places it at the location where $\xi' = 0$ on the second null or empty frequency plane, it will only receive the second term. Paying attention to lens L_3 completing the spacial integral for the coordinate x, the photoelectric receiving device is a square pattern wave detector, that is, it obtains the photoelectric receiving device's output electric current which is

$$\begin{aligned} i_d(t) \propto & \left| -\frac{1}{4}\tilde{a}_0 e^{-j2\pi(f+2f_0)t} \right. \\ & \left. \times \int_{-\frac{w}{2}}^{\frac{w}{2}} \tilde{a}_1(x-vt)\tilde{a}_2^*(x+vt)dx \right|^2 \\ \simeq & |\tilde{a}_0|^2 \cdot \tilde{r}_{12}(-2vt) \end{aligned} \tag{7}$$

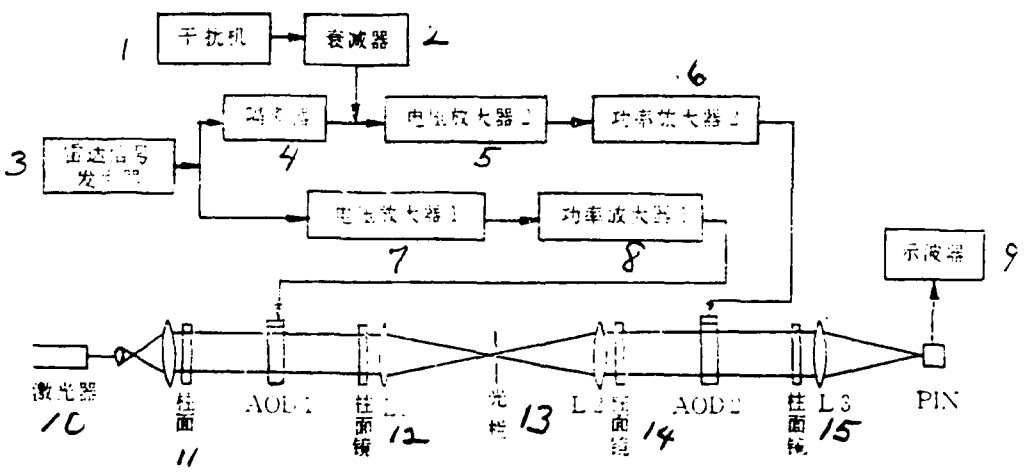

Fig. 2 Light Path and Circuit System for Experiments Using Spacial Integral Acousto-Optical Correlation Devices (1) Interference Mechanism (2) Attenuator (3) Radar Signal Generator (4) Isolator (5) Voltage Amplifier 2 (6) Power Amplifier 2 (7) Voltage Amplifier 1 (8) Power Amplifier 1 (9) Oscillascope (10) Laser (11) Rod Surface (12) Rod or Column Surface Lens (13) Diaphragm (14) Rod Surface Lens (15) Rod Surface Lens

In the equation

$$\tilde{r}_{12}(\tau) \equiv \int_{-\infty}^{+\infty} \tilde{a}_1(x)\tilde{a}_2^*(x-\tau)dx,$$

This is called the complex envelope correlation function. It is possible to demonstrate that it is a correlation function with the real signal

$$R_{12}(\tau) = \int_{-\infty}^{+\infty} s_1(t)s_2(t-\tau)dt$$

The relationship between them is

$$\begin{aligned} R_{12}(\tau) &= \frac{1}{2} R_e[\tilde{r}_{12}(\tau)e^{j2\pi f_0 \tau}] \\ &= \frac{1}{2} r_{12}(\tau)\cos\{2\pi f_0\tau \\ &\quad + \arg[\tilde{r}_{12}(\tau)]\} \end{aligned}$$

Comparing equation (7) and equation (3), it is possible to know that, due to the proportionality factors being, respectively, -2v and -v, it follows that the observed width of the correlation peak $i_a(t)$ and the pulse width of the signal s(t) are the same and it is not twice the pulse width of s(t).

III. Experimental Results

The light path system and circuit system used in the spacial integral acousto-optical correlation device employed in the experiments are as shown in Fig.2. The central frequency for the two acousto-optical devices was 110 MHz. The band width was $B \gtrsim 60$ MHz. The ultrasonic wave transit time was $T \gtrsim 4\,\mu s$. The rod or cylindrical lenses C_1-C_4 were used in order to take the laser bundle, after expanding and collimating it, and change it from a circular cross section to a long strip-shaped cross section in order to be

appropriate for application to the ultrasonic bundles with long, narrow shapes in the acousto-optical devices. Light barrier or diaphragm S stops the zero level light passing through AOD_1. It only lets the diffracted light of the null or empty frequency $\xi = \xi_0$ go through. As far as the point photoelectric receiving device formed by the PIN photoelectric diode being placed at the location where $\xi' = 0$ is concerned, it will only receive correlation quantities. The radar signals used were produced by the HL-11 model radar measuring instrument. The carrier frequency was adjustable. In line with this, we chose to set it at very slightly over a 3GHz position. The pulse was capable of varying from 0.5μs continuously to 2.5μs. The repetition frequency was also adjustable. However, when making tests, it was fixed at 3KHz. The amplitude of the output radar pulses could be continuously attenuated 50dB. The amount of attentuation was capable, on the instrumentation, of being read out continuously. The base oscillation was a continuous wave with a frequency equal to 3GHz. It was produced by an XFL-8 model centimeter wave signal generator. After going through frequency mixing in a 10 centimeter collector-mixer device, we obtained the center frequency signal of 110 MHz as the carrier frequency. After going through two voltage and power amplifier circuits, it was added to the two acousto-optical devices. In the experiments, the voltage amplitudes for the two radar pulse circuits were normally maintained at 1v. In the process of the tests, we also made use of two sets of HL-11 model radar measuring instruments to respectively produce the two radar circuit signals. However, the experimental results obtained were completely similar to the results when only one set was used. What the interference device produced was 3GHz wave band unmodulated random wave interference. It was easy to calculate. In Fig.2, the mixed frequency portion is not yet drawn out. In this way, with the addition of the electrical signal $s_1(t)$ onto AOD_1, it only contains the radar signal. It forms the reference signal. Moreover, with the addition of electrical signal $s_2(t)$ onto AOD_2, one, then, simultaneously, includes radar signals and random interference. It simulates actual band interference in returning radar wave signals received by radar antennas.

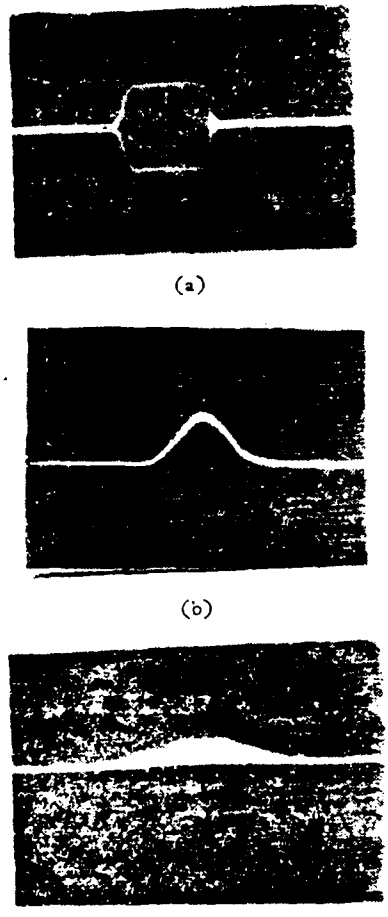

Figure 3.

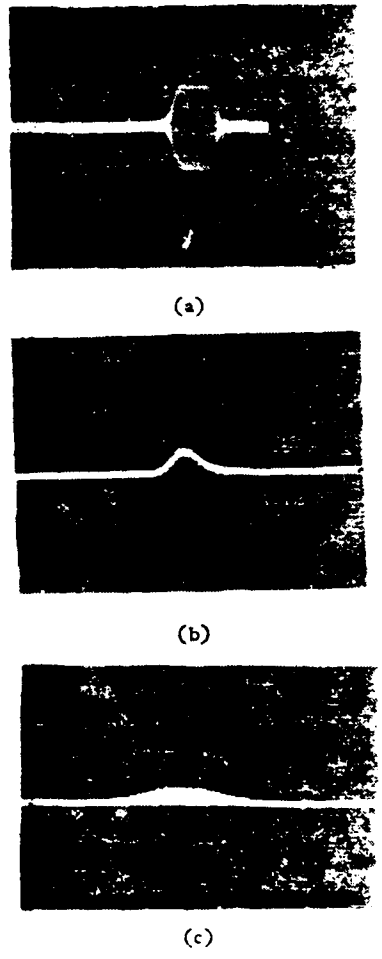

Figure 4.

Fig. 3 Radar Signals and Output Correlation Peaks When the Pulse Width Was 2μs. Horizontal Coordinates: 2μs/div (a) Radar Signal (1v/div); (b) Correlation Peak (200mv/div) When S/N = 0dB; (c) Correlation Peak (50mv/div) When S/N = -8dB

Fig. 4 Radar Signals and Output Correlation Peaks When the Pulse Width Was 1μs. Horizontal Coordinates: 2μs/div (a) Radar Signal (1v/div); (b) Correlation Peak (200mv/div) When S/N = 0dB; (c) Correlation Peak (50mv/div) When S/N =-8dB

1 表 1 实验数据

2 脉宽 (μs)	3 相关峰高度 (mV) $\frac{S}{N}=\infty$dB	$\frac{S}{N}=6$dB	$\frac{S}{N}=0$dB	$\frac{S}{N}=-6$dB	$\frac{S}{N}=-8$dB	4 相关增益 (dB)
0.5	60	40	35	2	15	23
1.0	120	90	70	40	30	26
1.5	200	120	100	60	40	28
2.0	240	180	150	80	60	29
2.5	300	220	160	100	70	30

Table 1 Experimental Data (2) Pulse (3) Correlation Peak Height (4) Correlation Gain

As far as the principal contents of the experiments are concerned, they are that, through adjustments, it was possible to change the attenuation device in order to alter the signal-to-noise ratio S/N for $s_2(t)$. We respectively measured the times when the S/N = ∞ dB (that is, the interference mechanism is turned off), 6dB, 0dB, -6dB, and -8dB, for the heights of the output correlation peaks. This experimental data is presented in Table 1. It should be pointed out that, when the S/N = 0dB, if one takes $s_2(t)$ and inputs it directly into an oscillascope for observation, in the background noise, it is still possible to make out the position of the radar pulse. Also, since this is the case, speaking from the angle of practical use, the signal at this time has still not been completely submerged by the noise. Going through a number of iterations of repeated measurements, one discovers that it does not matter how large the pulse width is. In all cases, when the S/N = -8dB, on the oscillascope, one directly observes $s_2(t)$, and the radar pulse has just been completely submerged in the background noise and cannot be redistinguished. On this basis, one again carries out another increase in the interference. One continues this straight on until the correlation peak completely disappears and then stops. From the readout of the variable attenuation device, at this time, one gets the dB number for the increase in interference. It is then possible to obtain the data in the last line of Table 1 "Correlation Gain". One

then repeats the measurements discussed above for different pulse widths. The results are all set out in Table 1. Fig.3 and Fig.4 are the correlation peak photographs for outputs when $s_2(t)$'s S/N = 0dB and -8dB as well as for radar signals when pulse widths are respectively equal to 2μs and 1μs.

From Table 1 and Fig.'s 3 and 4, it is possible to obtain the conclusions set out below: 1. Using this apparatus, it is possible to complete correlation reception. In conjunction with this, in a real time manner, one obtains entire correlation peaks. The correlation peak widths and the radar signal pulse widths were the same. This matches up with the theoretical analysis. 2. With the various types of S/N values, correlation peak heights all form a direct proportion with the pulse widths. Correlation gains also increase with increases in pulse width. It follows from this that correlation reception is quite appropriate for the relatively wide pulse widths of early warning radars. 3. Even if one is dealing with the simplest single-carrier-frequency, square-shaped pulse radar signals, acousto-optical correlation devices are still capable of obtaining relatively large correlation gains, which has practical value.

REFERENCES

[1] W.T. Maloney, IEEE Spectrum, 6-10 (1969), 40.

[2] R.A. Sprague, Opt. Eng. 16-5 (1977), 467.

[3] W.T. Rhodes, Proc. IEEE., 69 1 (1981), 65.

[4] M. Gottlieb, et al. Appl. Opt., 11 5 (1972) 1068

[5] C.J. Kramer, et al. Appl. Phys. Lett., 25 4 (1974), 180.

[6] N.J. Berg, et al, Proc. SPIE (Real Time Signal Processor), 154 1978, 181.

[7] N.J. Berg, et al. Appl. Opt., 18-16, (1979) 2767

[8] Xu Jieping; "The Precise Determination of Acousto-Optical Component Complex Transmission Rates" (awaiting publication)

DISTRIBUTION LIST

DISTRIBUTION DIRECT TO RECIPIENT

ORGANIZATION	MICROFICHE
A205 DMAHTC	1
C509 BALLISTIC RES LAB	1
C510 R&T LABS/AVEADCOM	1
C513 ARRADCOM	1
C535 AVRADCOM/TSARCOM	1
C539 TRASANA	1
C591 FSTC	4
C619 MIA REDSTONE	1
D008 MISC	1
E053 HQ USAF/INET	1
E404 AEDC/DOF	1
E408 AFWL	1
E410 AD/IND	1
F429 SD/IND	1
P005 DOE/ISA/DDI	1
P050 CIA/OCR/ADD/SD	2
AFIT/LDE	1
NOIC/OIC-9	1
CCV	1
MIA/PHS	1
LLYL/CODE L-309	1
NASA/NST-44	1
NSA/T513/TDL	2
ASD/FTD/TQIA	1
FSL	1